

Effects of the molecular weight of molecular chains constituting the reaction medium on the thermal degradation of polyisobutylene

Takashi Sawaguchi* and Manabu Seno

Department of Industrial Chemistry, College of Science and Technology, Nihon University, Kandasurugadai, Chiyoda-ku, Tokyo, 101 Japan

(Received 23 June 1997; revised 7 August 1997; accepted 22 September 1997)

Non-volatile oligomers obtained by the thermal degradation of polyisobutylene were finely fractionated and the distribution of the functional groups of each fraction was characterized by a kinetic approach including the intermolecular hydrogen abstraction of primary and tertiary terminal macroradicals ($R_p\cdot$ and $R_t\cdot$) and volatile small radicals ($S\cdot$), followed by β scission. The observed value of the composition ratio $[TTD]/[NTTD]$, which is related to the ratio of the competitive β scission rates of a secondary on-chain macroradical, increases monotonically with decreasing molecular weight (M) of the fractions. This result shows clearly that the reactivity for β scission depends on the segmental motion of the reacting radicals. With respect to the composition ratio $[t\text{-Bu}]/[iPr]$, which is related to the concentration ratio $[R_p\cdot]/[R_t\cdot]$, the observed value is roughly constant with M for $M > M_c$, but decreases with decreasing M for $M < M_c$, where M_c corresponds approximately to the characteristic molecular weight for the entanglement of molten polymer. This ratio for $M > M_c$ decreases with decreasing average molecular weight of the molten polymer matrix, owing to an increase in the rate of diffusion-controlled termination. For $M < M_c$, the value of the exponent a determined from the slope of the double logarithmic plots of $[t\text{-Bu}]/[iPr]$ against M is about 0.5 in all cases. This suggests that the hydrogen abstraction of $S\cdot$ depends on the chain dimension of unentangled polymer. It is confirmed from these results that the degradation reaction of all the polymer molecules in an homogenous reaction medium is entirely affected by the segmental motion and self-diffusional motion of the degrading polymers, and the effect of the chain dimension is observed only for unentangled polymer molecules during the degradation. © 1998 Elsevier Science Ltd. All rights reserved.

(Keywords: polymer melt; thermal degradation; polyisobutylene)

LIST OF ABBREVIATIONS

iPr	isopropyl end-group, or polymer having iPr
m	monomer or its molecular weight
<i>t</i> -Bu	<i>tert</i> -butyl end-group, or polymer having <i>t</i> -Bu
NTTD	non-terminal trisubstituted double bond, or polymer having NTTD
NTVD	non-terminal vinylidene double bond, or polymer having NTVD
P	polymer molecule
$R_{oi1}\cdot$	primary on-chain macroradical
$R_{oi2}\cdot$	secondary on-chain macroradical
$R_p\cdot$	primary (p) terminal macroradical
$[R_p\cdot]$	integrated concentration of $R_p\cdot$: $\int [R_p\cdot] dt$
$R_t\cdot$	tertiary (t) terminal macroradical
$[R_t\cdot]$	integrated concentration of $R_t\cdot$: $\int [R_t\cdot] dt$
$S\cdot$	volatile small radical
$[S\cdot]$	integrated concentration of $S\cdot$: $\int [S\cdot] dt$
SH	volatiles and semi-volatile oligomers
TTD	terminal trisubstituted double bond, or polymer having TTD
TVD	terminal vinylidene double bond, or polymer having TVD

INTRODUCTION

Many attempts have been made to elucidate the effects of the polymer dynamics on polymer reactions. In particular, diffusion-controlled termination in free-radical

polymerization was analyzed based on an interpolymer reaction model¹, and the effects of diffusion of the reacting polymer molecules as well as their molecular weight and solvent were clarified². Mita and Horie³ reviewed the effects of the molecular weight of polymer molecules and the translational diffusion of the polymer segment on polymer reactions in solution, and the effect of the secondary transition on polymer reactions in the bulk, but little is known about these effects on polymer reactions in the melt.

The molecular weight should affect strongly the polymer reactions in the melt, such as the thermal degradation of the polymers⁴, although this is not yet well understood. In the present series of studies^{5–12}, we attempt to elucidate the effect of molecular weight on the elementary reactions of the thermal degradation of polyisobutylene from structural and kinetic analyses of the products, which consist of gaseous compounds containing mainly the isobutylene monomer, and volatile and non-volatile oligomers. The results obtained hitherto are summarized as follows.

The products are mainly derived from $R_p\cdot$, $R_t\cdot$, and $S\cdot$ (see List of Abbreviations) in the depropagation step of the radical chain mechanism^{5–9}. The depolymerization (direct β scission) of $R_p\cdot$ and $R_t\cdot$ leading to the formation of isobutylene monomer depends on the height of the energy barrier of rotation around the C–C \cdot bond of these macroradicals; that is, the higher rate constant of β scission of $R_t\cdot$ than that of $R_p\cdot$ is caused by the higher energy barrier of rotation of the former than that of the latter¹¹. Moreover,

* To whom correspondence should be addressed

the intramolecular hydrogen abstraction (back-biting) of $R_p\cdot$ and $R_t\cdot$ followed by β scission at the inner position of the main chain lead to the formation of four types of monoolefins, which are the main components of the volatile oligomers. This back-biting proceeds according to unimolecular reaction kinetics and is scarcely affected by the considerable decrease in the molecular weight of the molten polymer matrix which forms the reaction medium during the degradation, depending only on the local motion (chain conformation) of the chain-end radicals^{6,7}.

On the other hand, it could be deduced from other kinetic considerations of back-biting that the decrease in the molecular weight of the molten polymer matrix leads to a decrease in the integrated macroradical concentration ratio $[R_p\cdot]/[R_t\cdot]$ ^{7,8}. Although the non-volatile oligomers are formed by intermolecular hydrogen abstraction followed by β scission, it was shown clearly that a similar trend in the decrease of the ratio $[R_p\cdot]/[R_t\cdot]$ is obtained from the composition ratio between functional groups of interest in the non-volatile oligomers^{9,10}. Thus, the products of the degradation were successfully simulated according to the total reaction model which includes diffusion-controlled termination, when the value of the exponent a is assigned to be about 2^{13} for the power law of the molecular weight dependence of the self-diffusional motion of the reacting radical in the molten polymer matrix¹⁰. The rate of decrease in the concentration is estimated to follow the order $S \cdot > R_p \cdot \gg R_t \cdot$. This order results from an increase in the rate of termination with decreasing molecular weight of the molten polymer matrix as the reaction proceeds.

In this paper, the non-volatile oligomers formed by the thermal degradation of polyisobutylene are precisely fractionated by gel permeation chromatography (g.p.c.), and the distribution of functional groups in each fraction is determined by n.m.r. spectroscopy. Therefore, the effect of the molecular weight of the molecular chains constituting the reaction medium on the composition ratios of the functional groups is examined, and the dynamic behaviour of the unentangled and entangled molten polymer chains affecting the elementary reactions is discussed.

EXPERIMENTAL

Sample, apparatus and procedure

The polyisobutylene sample and the experimental procedure are described in detail elsewhere⁵. Molecular weight characteristics of the purified polyisobutylene are as follows: $M_n = 2.5 \times 10^5$ and $M_w/M_n = 2.50$. A 1 g amount of sample was used for each degradation experiment at 300 or 320°C. After the degradation reaction, the polymer residue in the reaction flask was dissolved in 10 cm³ of chloroform and was reprecipitated by dropping the solution into 50 cm³ of acetone in order to remove the small amount of semi-volatile oligomers with a relatively low volatility. The reprecipitates, which are termed the non-volatile oligomers, were analyzed after vacuum drying under heating.

G.p.c.

The fractionation of the non-volatile oligomers and the measurements of the molecular weight dispersion (M_w/M_n) were performed on a gel permeation chromatograph (Toyo Soda HLC-802 UR) using a stainless-steel column of TSK-GEL (2 × HMG6 + H4000HG8 + H2000HG8).

Molecular weight

The M_n of the non-volatile oligomers was determined by the following equation¹⁴, using the limiting viscosity $[\eta]$ (dm³ g⁻¹) measured at 30°C in toluene: $[\eta] = 3.71 \times 10^{-4} P^{0.75}$. In this equation, P is the number-average degree of polymerization determined by the osmotic pressure method. The M_n and M_w of the fractionated oligomers were calculated from the following equations: $M_n = 278.1 + A_n \times 27.38$ (coefficient of correlation, 0.9626) and $M_w = 293.8 + A_w \times 28.17$ (coefficient of correlation, 0.9711), where A_n and A_w are the number- and weight-average chain lengths, respectively, calibrated using the values of M_n/Q and M_w/Q of the polystyrene standard for g.p.c. measurements, respectively, employing a Q factor of 41. These relationships were estimated by checking the plots of M_n (from $[\eta]$) vs. A_n and M_w ($M_n \times A_w/A_n$) vs. A_w for over 100 samples of non-volatile oligomers⁵⁻¹² having M_n values ranging from 8×10^2 to 2.1×10^4 by the least-squares method.

N.m.r.

The 400 MHz ¹H n.m.r. spectra were obtained with use of a Jeol JNM-GX400 spectrometer operating at 399.65 MHz and at room temperature with an internal lock. The sample concentration was approximately 10% (w/v) in chloroform-*d*₁. Tetramethylsilane (TMS) was used as internal standard and 5 mm diameter sample tubes were employed. The spectral width was 4.5 kHz, and 65 536 data points were accumulated in a JEC 32 computer. In the quantitative measurements⁸, a pulse width of 90° (approximately 11.7 μs) and a pulse repetition time of 37.281 s were adopted. A typical measurement was performed over about 10–45 h. The signal intensities in the spectra were measured by the area method. The composition of the functional groups was determined from the intensities of the signals of the corresponding methyl group protons⁸.

RESULTS AND DISCUSSION

Molecular characteristics of the fractionated oligomers

As described in previous papers⁵⁻¹², the yield of the volatiles including gaseous compounds and volatile oligomers increases and the polymer residue constituting the reaction medium decreases during thermal degradation at 300 or 320°C. Molecular weight characteristics of the non-volatile oligomers isolated from the polymer residue and

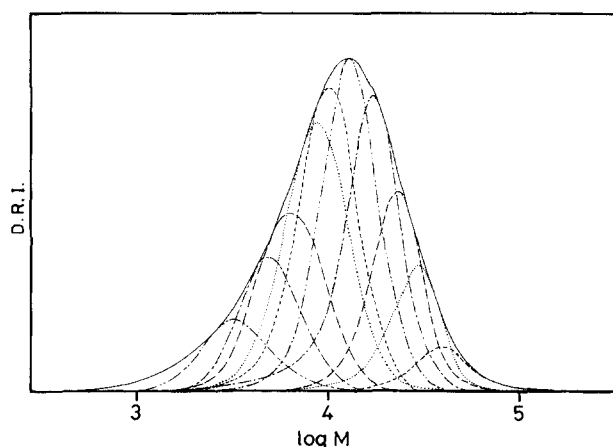


Figure 1 An example of g.p.c. curves for the non-volatile oligomers and their fractionated samples

Table 1 Molecular weight characteristics of fractions resulting from non-volatile oligomers obtained by thermal degradation of polyisobutylene ($M_n = 2.50 \times 10^5$) at 300°C

Time (min)	Fraction no.	M_w/M_n^a	$10^{-3} M_n^b$	$10^{-3} M_w^c$	$10^{-3} M_w^b$
180	Whole	1.87	8.74	16.4	16.6
	F1	1.06	32.4	34.3	35.2
	F2	1.07	24.4	26.1	26.9
	F3	1.06	20.6	21.9	22.5
	F4	1.07	18.1	19.3	19.9
	F5	1.08	15.2	16.5	16.9
	F6	1.09	12.3	13.4	13.83
	F7	1.12	9.89	11.0	11.33
	F8	1.12	7.18	8.03	8.24
	F9	1.15	4.71	5.39	5.51
	F10	1.31	2.30	3.02	3.03
300	Whole	1.73	6.93	12.0	12.1
	F1	1.04	27.2	28.3	29.0
	F2	1.05	21.5	22.5	23.2
	F3	1.04	18.8	19.6	20.2
	F4	1.05	15.4	16.2	16.7
	F5	1.06	12.0	12.7	13.0
	F6	1.06	9.28	9.85	10.1
	F7	1.07	7.29	7.81	8.03
	F8	1.09	5.23	5.68	5.83
	F9	1.11	3.45	3.84	3.92
	F10	1.16	1.94	2.24	2.27

^aEquals the values of A_w/A_n determined by g.p.c. measurements

^bCalculated from the following equations: $M_n = 278.1 + A_n \times 27.38$, or $M_w = 293.8 + A_n \times 28.17$; estimated from the plots of average molecular length (A) vs. average molecular weight (M)

^c $M_n \times (M_w/M_n)$

their fractionated samples are given in *Table 1* and *Table 2*. An example of g.p.c. curves of the non-volatile oligomers and their fractions is shown in *Figure 1*. As shown in *Tables 1 and 2*, the M_n values of the non-volatile oligomers decrease with an increase in reaction time at both temperatures. *Figure 1* shows that each of the fractionated samples is properly separated from the whole of the non-volatile oligomers. All the fractionated oligomers maintain a sharp molecular weight dispersion (M_w/M_n) of about 1.1–1.2 (*Tables 1 and 2*).

The functionality of the functional groups (*t*-Bu, *i*Pr, TVD, TTD and NTTD) is defined as the average number of a given functional group per molecule, and is calculated by the following equation, assuming all the non-volatile oligomers are linear⁸.

$$f = \frac{2 \times (\text{signal intensity of the functional group of interest})}{(\text{signal intensity of all end-groups, i.e. } i\text{Pr} + t\text{-Bu} + \text{TTD} + \text{TVD})}$$

The composition and functionality of each of the end-groups and double bonds of the non-volatile oligomers and their fractionated samples at 300 and 320°C are listed in *Tables 3 and 4*. The functionalities f_t and f_{in} in *Tables 3 and 4* represent the average number of terminal double bonds and the average total number of double bonds per molecule, respectively. With respect to the fractionated oligomers, f_{in} decreases clearly with decreasing M of the fractions at both temperatures, and this is caused mainly by a decrease in f_{NTTD} . Other functionalities f_{iPr} , f_{t-Bu} , f_{TTD} , f_{TVD} and f_t change in a complicated way with the M of the fractions.

Composition ratio and kinetic equation

In a previous paper⁸, reasonable elementary reactions were proposed for the formation of the functional groups; intermolecular hydrogen abstractions of radicals give two types of on-chain macroradicals ($R_{oi1}\cdot$ and $R_{oi2}\cdot$), depending on the position (CH_3 or CH_2) of hydrogen abstraction, independently of the radical type. Moreover, hydrogen abstractions of $R_p\cdot$, $R_t\cdot$ and $S\cdot$ yield *t*-Bu, *i*Pr and SH (volatiles), respectively. The β scission of $R_{oi1}\cdot$ occurs only at the main chain, not at the side methyl group, and results exclusively in the formation of TVD and $R_p\cdot$, not NTTD and the methyl radical. On the other hand, the β scission of $R_{oi2}\cdot$ produces TTD and $R_p\cdot$ or NTTD and the methyl radical, depending on the positions (main chain or side methyl group) of scission.

According to the reaction model described above, the formation of each functional group of the non-volatile oligomers was analyzed kinetically, assuming that the reactions occur competitively at the steady state where the concentrations of the on-chain macroradicals ($R_{oi1}\cdot$ and $R_{oi2}\cdot$) are kept low and constant. The molar concentrations of the respective functional groups formed for a given time were obtained by integration⁹. The mechanism of the formation of these functional groups is examined by analyzing the observed values of the ratios between the compositions of the respective functional groups by the

Table 2 Molecular weight characteristics of the fractions resulting from non-volatile oligomers obtained by the thermal degradation of polyisobutylene ($M_n = 2.50 \times 10^5$) at 320°C

Time (min)	Fraction no.	M_w/M_n^a	$10^{-3} M_n^b$	$10^{-3} M_w^c$	$10^{-3} M_w^b$
15	Whole	1.86	11.4	21.2	21.6
	F1	1.08	37.3	40.3	41.4
	F2	1.07	27.6	29.5	30.3
	F3	1.10	21.5	23.7	24.3
	F4	1.11	16.4	18.2	18.8
	F5	1.12	12.1	13.6	14.0
	F6	1.15	7.42	8.53	8.73
30	Whole	2.16	6.73	14.5	14.6
	F1	1.16	35.0	40.6	41.7
	F2	1.16	24.9	28.9	29.7
	F3	1.13	20.9	23.6	24.2
	F4	1.26	13.7	17.3	17.7
	F5	1.16	11.7	13.6	13.9
	F6	1.20	8.64	10.4	10.6
	F7	1.20	7.65	9.18	9.36
	F8	1.20	5.68	6.82	6.95
	F9	1.16	4.59	5.32	5.44
120	Whole	1.56	3.07	4.78	4.77
	F1	1.08	7.33	7.92	8.12
	F2	1.08	5.64	6.09	6.23
	F3	1.09	4.22	4.60	4.71
	F4	1.08	3.21	3.47	3.56
	F5	1.08	2.46	2.66	2.71
	F6	1.10	1.77	1.95	1.98

^aEqual to the values of A_w/A_n determined by g.p.c. measurements

^bCalculated from the following equations: $M_n = 278.1 + A_n \times 27.38$, or $M_w = 293.8 + A_n \times 28.17$; estimated from the plots of average molecular length (A) vs. average molecular weight (M)

^c $M_n \times (M_w/M_n)$

kinetic equations leading to the corresponding ratios⁹. These relationships are given as follows

$$\frac{[t\text{-Bu}]}{[i\text{Pr}]} \propto \frac{(k_{pi1} + k_{pi2})[\mathbf{R}_p\cdot]}{(k_{ti1} + k_{ti2})[\mathbf{R}_t\cdot]} \quad (1)$$

$$\frac{[\text{TTD}] + [\text{NTTD}]}{[\text{TVD}]} \propto \frac{k_{pi2}[\mathbf{R}_p\cdot] + k_{ti2}[\mathbf{R}_t\cdot] + k_{vi2}[\mathbf{S}\cdot]}{k_{pi1}[\mathbf{R}_p\cdot] + k_{ti1}[\mathbf{R}_t\cdot] + k_{vi1}[\mathbf{S}\cdot]} \quad (2)$$

$$\frac{[\text{TTD}]}{[\text{NTTD}]} \propto \frac{k_{si2}}{k_{si2m}} \quad (3)$$

The ratio $[t\text{-Bu}]/[i\text{Pr}]$ is expressed as the product of the ratio of the rate constants and the ratio $[\mathbf{R}_p\cdot]/[\mathbf{R}_t\cdot]$, equation (1). Thus, a change of $[t\text{-Bu}]/[i\text{Pr}]$ reflects sensitively that of the macroradical concentration ratio during the degradation. On the other hand, the ratio $([\text{TTD}] + [\text{NTTD}])/[\text{TVD}]$ is expressed in terms of a ratio including the abstraction rates of different types of hydrogen species (CH_2 and CH_3) of $\mathbf{R}_p\cdot$, $\mathbf{R}_t\cdot$ and $\mathbf{S}\cdot$, as given in equation (2), and it is proportional to the ratio of the on-chain macroradical concentration ($[\mathbf{R}_{oi2}\cdot]/[\mathbf{R}_{oi1}\cdot]$). The ratio $[\text{TTD}]/[\text{NTTD}]$ is expressed only as the rate constant ratio of the competitive β scissions of $\mathbf{R}_{oi2}\cdot$, equation (3).

Effect of molecular weight on the composition ratio, $[t\text{-Bu}]/[i\text{Pr}]$

The values of $[t\text{-Bu}]/[i\text{Pr}]$ of the non-volatile oligomers

calculated from the respective compositions (Tables 3 and 4) are 12.7 and 8.91 for 180 min and 300 min at 300°C, and 27.2, 16.2 and 8.22 for 15 min, 30 min and 120 min at 320°C, respectively. At both temperatures, the ratio $[t\text{-Bu}]/[i\text{Pr}]$ decreases clearly with degradation time, owing to the decreasing ratio of $[\mathbf{R}_p\cdot]/[\mathbf{R}_t\cdot]$. This is supported by the simulation result that the rate of decrease in the concentration follows the order $\mathbf{R}_p\cdot \gg \mathbf{R}_t\cdot$, resulting from an increase in the rate of self-diffusion-controlled termination with decreasing average molecular weight of the molten polymer matrix as the reaction proceeds^{9,10}.

For the fractionated oligomers, plots of the ratio $[t\text{-Bu}]/[i\text{Pr}]$ against M of the fractions are shown in Figure 2a (300°C) and Figure 2b (320°C), where the g.p.c. curves are illustrated as a function of reaction time. Surprisingly, this ratio does not keep to a constant value over the whole range of molecular weights for respective non-volatile oligomers at both temperatures, although a constant value is expected exclusively for the ratio between the rates of elementary reactions in the homogeneous reaction medium. As shown in Figure 2, the ratio $[t\text{-Bu}]/[i\text{Pr}]$ decreases markedly with decreasing M of the fractions when the value of M is smaller than 1×10^4 – 2×10^4 . This decrease in $[t\text{-Bu}]/[i\text{Pr}]$ means that the distribution of the concentrations of individual $\mathbf{R}_p\cdot$ and $\mathbf{R}_t\cdot$ depends on the M of the molecular chains in the molten polymer matrix. If this result is caused by an increase in the rate of diffusion-controlled termination with

Table 3 Composition and functionality of respective end-groups and double bonds of fractions resulting from the non-volatile oligomers obtained by the thermal degradation of polyisobutylene at 300°C

Time (min)	Fraction no.	Composition ^a (mol%)					Functionality ^b						
		[iPr] ^c	[<i>t</i> -Bu] ^d	[TTD] ^e	[TVD] ^f	[NTTD] ^g	<i>f</i> _{iPr}	<i>f</i> _{<i>t</i>-Bu}	<i>f</i> _{TTD}	<i>f</i> _{TVD}	<i>f</i> _{NTTD}	<i>f</i> _t ^h	<i>f</i> _n ⁱ
180	Whole	1.41	17.90	51.62	18.72	10.35	0.031	0.399	1.15	0.418	0.231	1.57	1.80
	F1	0.68	15.40	48.20	18.53	17.20	0.016	0.372	1.16	0.448	0.415	1.61	2.03
	F2	0.61	14.16	51.16	18.82	15.25	0.014	0.334	1.21	0.444	0.360	1.65	2.01
	F3	0.58	13.31	51.49	19.19	15.43	0.014	0.315	1.22	0.454	0.365	1.67	2.04
	F4	0.59	13.36	52.89	18.91	14.24	0.014	0.312	1.23	0.441	0.332	1.68	2.01
	F5	0.60	13.15	53.69	19.50	13.06	0.014	0.303	1.24	0.449	0.300	1.68	1.98
	F6	0.65	12.75	54.75	19.77	12.08	0.015	0.290	1.25	0.450	0.275	1.70	1.97
	F7	0.75	12.26	55.50	19.94	11.55	0.017	0.277	1.26	0.451	0.261	1.71	1.97
	F8	0.84	12.24	55.29	20.49	11.14	0.019	0.275	1.24	0.461	0.251	1.71	1.96
	F9	1.11	13.63	54.81	20.46	9.99	0.025	0.303	1.22	0.455	0.222	1.67	1.89
300	Whole	2.01	17.90	52.73	15.97	11.39	0.045	0.404	1.19	0.360	0.257	1.55	1.81
	F1	0.99	15.15	47.91	15.25	20.70	0.025	0.382	1.21	0.385	0.522	1.59	2.12
	F2	1.03	15.71	49.53	15.80	17.93	0.025	0.383	1.21	0.385	0.437	1.59	2.03
	F3	1.07	14.60	51.29	16.36	16.68	0.026	0.350	1.23	0.393	0.400	1.62	2.02
	F4	1.01	14.00	52.92	16.48	15.59	0.024	0.332	1.25	0.390	0.369	1.64	2.01
	F5	1.00	13.50	54.54	16.90	14.06	0.023	0.314	1.27	0.393	0.327	1.66	1.99
	F6	1.01	13.39	55.10	17.00	13.50	0.023	0.310	1.27	0.393	0.312	1.67	1.98
	F7	1.12	13.48	54.85	17.54	13.01	0.026	0.310	1.26	0.403	0.299	1.66	1.96
	F8	1.32	14.63	54.62	17.23	12.20	0.030	0.333	1.24	0.392	0.278	1.64	1.92
	F9	2.02	17.13	53.94	17.01	9.89	0.045	0.380	1.20	0.378	0.220	1.58	1.79
	F10	4.76	28.67	44.98	14.45	7.14	0.103	0.617	0.97	0.311	0.154	1.28	1.43

^a100 × (each CH₃ peak intensity/total CH₃ signal intensity : iPr + *t*-Bu + TTD + TVD + NTTD)

^bAverage number of each functional group per molecule: $f = 2 \times (\text{each functional group peak intensity}) / (\text{total terminal peak intensity})$: iPr + *t*-Bu + TTD + TVD)

^cIsopropyl: (CH₃)₂CH-

^d*tert*-Butyl: (CH₃)₃C-

^eTerminal trisubstituted double bond: (CH₃)₂C=CH-

^fTerminal vinylidene double bond: CH₂=C(CH₃)-

^gNon-terminal trisubstituted double bond: -(CH₃)₂C=CH-

^hAverage number of terminal double bonds per molecule: $f_t = 2 \times ([TTD] + [TVD]) / ([iPr] + [t-Bu] + [TTD] + [TVD])$

ⁱAverage total number of double bonds per molecule: $f_n = 2 \times ([TTD] + [TVD] + [NTTD]) / ([iPr] + [t-Bu] + [TTD] + [TVD])$

a decrease in *M* of the fractions, the reaction medium constituted of molten polymer molecules should be phase-separated, depending on *M*. However, the reaction medium is an homogeneous phase, as is described later, and therefore this change in the concentration ratio [R_p·]/[R_t·] should result from changes in the rates of the elementary reactions, depending on the physical properties of the reaction medium affected by *M*. The *M* dependence of the ratio [R_p·]/[R_t·] is discussed in detail in the following section.

$([TTD] + [NTTD])/[TVD]$

Plots of the composition ratio $([TTD] + [NTTD])/[TVD]$ against *M* of the fractionated oligomers are shown in Figure 3a (300°C) and Figure 3b (320°C). The composition ratio gradually decreases with decreasing *M* and increases with increase in reaction time at both temperatures. Since the ratio $([TTD] + [NTTD])/[TVD]$ is expressed in terms of the ratio of the abstraction rates (sum) of the different types of hydrogen atoms of the respective radicals, this ratio is insensitive to a small change in the radical concentration ratio. In a previous paper¹⁰, it was expected that at an earlier stage of the reaction [R_p·] and [R_t·] are larger than [S·]. Moreover, the rate of decrease in concentration follows the order S· > R_p· ≫ R_t· during the degradation, and [R_p·] is slightly lower than [R_t·] in the range of *M*_n below about

1 × 10⁴. Such a larger change in the radical concentration ratio is reflected in a higher value of this ratio for the non-volatile oligomers obtained for 120 min at 320°C, which consist only of molecular chains having *M* below about 1 × 10⁴ (Figure 3b). This is based on the deduction that the ratio of the abstraction rate constants of R_t· is larger than those of R_p· and S·. Therefore, the present experimental results suggest that the non-volatile oligomers form an homogeneous reaction matrix and the mean concentration ratio of the respective radicals is regulated by the relative ratio of the rates of the elementary reactions, depending on the average molecular weight of the molten polymer matrix.

$[TTD]/[NTTD]$

Figure 4a and 4b show plots of the composition ratio [TTD]/[NTTD] against *M* of the fractionated oligomers at 300 and 320°C, respectively. The ratio is expressed only by the rate constant ratio of the competitive β scissions of R_{oi2}·, independently of the concentration (equation (3)). Against expectations, this ratio increases clearly with decreasing *M* of the non-volatile oligomers at both temperatures (Figure 4). This tendency should be interpreted by a hypothesis that the rate constant ratio of β scissions of R_{oi2}· depends on *M*.

In a previous paper¹¹, we reported that the rate of depolymerization (direct β scission) of R_p· and R_t·, leading

Table 4 Composition and functionality of respective end-groups and double bonds of fractions resulting from the non-volatile oligomers obtained by the thermal degradation of polyisobutylene at 320°C

Time (min)	Fraction no.	Composition ^a (mol%)					Functionality ^b							
		[iPr] ^c	[<i>t</i> -Bu] ^d	[TTD] ^e	[TVD] ^f	[NTTD] ^g	<i>f</i> _{iPr}	<i>f</i> _{<i>t</i>-Bu}	<i>f</i> _{TTD}	<i>f</i> _{TVD}	<i>f</i> _{NTTD}	<i>f</i> _t ^h	<i>f</i> _u ⁱ	
15	Whole	0.63	17.11	49.15	22.15	10.96	0.014	0.384	1.10	0.498	0.246	1.60	1.85	
	F1	0.47	14.00	44.80	20.70	20.03	0.012	0.350	1.12	0.518	0.501	1.64	2.14	
	F2	0.42	12.94	48.56	21.28	16.80	0.010	0.311	1.17	0.512	0.404	1.68	2.08	
	F3	0.53	15.20	49.46	23.40	14.41	0.012	0.343	1.12	0.528	0.325	1.64	1.97	
	F4	0.41	11.56	52.82	22.28	12.93	0.009	0.266	1.21	0.512	0.297	1.73	2.02	
	F5	0.46	12.28	52.28	22.91	12.07	0.010	0.279	1.19	0.521	0.275	1.71	1.98	
	F6	0.65	12.84	52.33	22.90	11.28	0.015	0.289	1.18	0.516	0.254	1.70	1.95	
30	Whole	0.92	14.88	50.82	20.44	12.94	0.021	0.342	1.17	0.470	0.297	1.64	1.93	
	F1	0.67	11.98	47.14	18.60	21.62	0.017	0.306	1.20	0.475	0.552	1.68	2.23	
	F2	0.79	12.77	47.80	18.58	20.06	0.020	0.319	1.20	0.465	0.502	1.66	2.16	
	F3	0.63	13.96	51.23	17.99	16.19	0.015	0.333	1.22	0.429	0.386	1.65	2.04	
	F4	0.64	11.37	51.22	19.76	17.01	0.015	0.274	1.23	0.476	0.410	1.71	2.12	
	F5	0.75	13.76	48.62	21.48	15.39	0.018	0.325	1.15	0.508	0.364	1.66	2.02	
	F6	0.56	10.89	52.76	21.35	14.44	0.013	0.255	1.23	0.499	0.338	1.73	2.07	
	F7	0.75	12.43	55.48	20.06	11.27	0.017	0.280	1.25	0.452	0.254	1.70	1.96	
	F8	0.70	11.74	56.12	21.00	10.44	0.016	0.262	1.25	0.469	0.233	1.72	1.96	
	F9	0.81	11.39	55.18	21.67	10.95	0.018	0.256	1.24	0.487	0.246	1.68	1.97	
F10	1.34	14.75	53.52	20.64	9.75	0.030	0.327	1.19	0.457	0.216	1.64	1.86		
120	Whole	2.40	19.72	53.46	10.43	14.00	0.056	0.459	1.24	0.243	0.326	1.49	1.81	
	F1	1.90	16.74	51.09	10.63	19.64	0.047	0.417	1.27	0.265	0.489	1.54	2.02	
	F2	2.04	16.14	53.42	10.77	17.63	0.050	0.392	1.30	0.262	0.428	1.56	1.99	
	F3	2.39	15.83	54.60	11.11	16.06	0.057	0.377	1.30	0.265	0.383	1.57	1.95	
	F4	2.64	15.65	54.93	11.20	15.58	0.063	0.371	1.30	0.265	0.369	1.57	1.94	
	F5	3.13	17.23	53.91	11.15	14.58	0.073	0.403	1.26	0.261	0.341	1.52	1.86	
F6	5.24	23.03	49.42	10.93	11.39	0.118	0.520	1.12	0.247	0.247	1.36	1.62		

^a100 × (each CH₃ peak intensity/total CH₃ signal intensity : iPr + *t*-Bu + TTD + TVD + NTTD)^bAverage number of each functional group per molecule: $f = 2 \times (\text{each functional group peak intensity}) / (\text{total terminal peak intensity : iPr} + \textit{t}\text{-Bu} + \text{TTD} + \text{TVD})$ ^cIsopropyl: (CH₃)₂CH-^d*tert*-Butyl: (CH₃)₃C-^eTerminal trisubstituted double bond: (CH₃)₂C=CH-^fTerminal vinylidene double bond: CH₂=C(CH₃)-^gNon-terminal trisubstituted double bond: -(CH₃)C=CH-^hAverage number of terminal double bonds per molecule: $f_t = 2 \times ([\text{TTD}] + [\text{TVD}]) / ([\text{iPr}] + [\textit{t}\text{-Bu}] + [\text{TTD}] + [\text{TVD}])$ ⁱAverage number of total double bonds per molecule: $f_u = 2 \times ([\text{TTD}] + [\text{TVD}] + [\text{NTTD}]) / ([\text{iPr}] + [\textit{t}\text{-Bu}] + [\text{TTD}] + [\text{TVD}])$

to the formation of isobutylene monomer, depends on the energy barrier of rotation around the C-C· bond of these macroradicals. This is based on an idea that β scission takes place just when the C-C bond of interest is properly aligned with the p-orbital of the carbon radical and depends on the rotation around the C-C· bond¹¹. A Newman projection diagram of the rotational isomeric state of the C-C· bond of R_{oi1}· and R_{oi2}· favourable for the β scission is shown in Figure 5. The β scission of R_{oi1}· leads to the formation of TVD and R_p· via conformer I, and NTVD and the methyl radical via conformer II. On the other hand, the experimental results showed that NTVD was not produced but only TVD⁸. The geometry of R_{oi1}· is extremely similar to R_p· and therefore the C-C· bond of R_{oi1}· rotates freely at higher temperatures, owing to the low energy barrier of rotation of R_p·¹¹. Consequently, β scission would take place exclusively via conformer I, and the probability of occurrence via conformer I is at least twice as large as that via conformer II, as shown in Figure 5.

On the other hand, it is deduced from the results of the calculation of the conformational energy of the C-C· bond of R_t·¹¹ that the R_{oi2}· radical has two types of the most stable

conformers, III and IV, which correspond to the eclipsed conformations where C· is properly aligned with the β-bond. The β scission of R_{oi2}· occurs more frequently because of the high probability of occurrence of the conformer having the eclipsed conformation, in contrast to R_{oi1}·. According to this concept, the present results show clearly that the decrease in the probability of occurrence of the conformer IV rather than the conformer III results from a decrease in *f*_{NTTD} with decreasing *M* (Tables 3 and 4). This indicates that the rate constant (*k*_{si2m}) of β scission of R_{oi2}· at the position of the side methyl group decreases relatively, owing to an increase in the segmental mobility of the reacting molecules with decreasing *M*.

Molecular weight dependence of [*t*-Bu]/[iPr]

The molecular weight dependence of the ratio [R_p·]/[R_t·] can be estimated from the composition ratio [*t*-Bu]/[iPr], as follows^{7,9}

$$\frac{[\text{R}_p\cdot]}{[\text{R}_t\cdot]} \propto \frac{[\textit{t}\text{-Bu}]}{[\text{iPr}]} \propto M_n^a \quad (4)$$

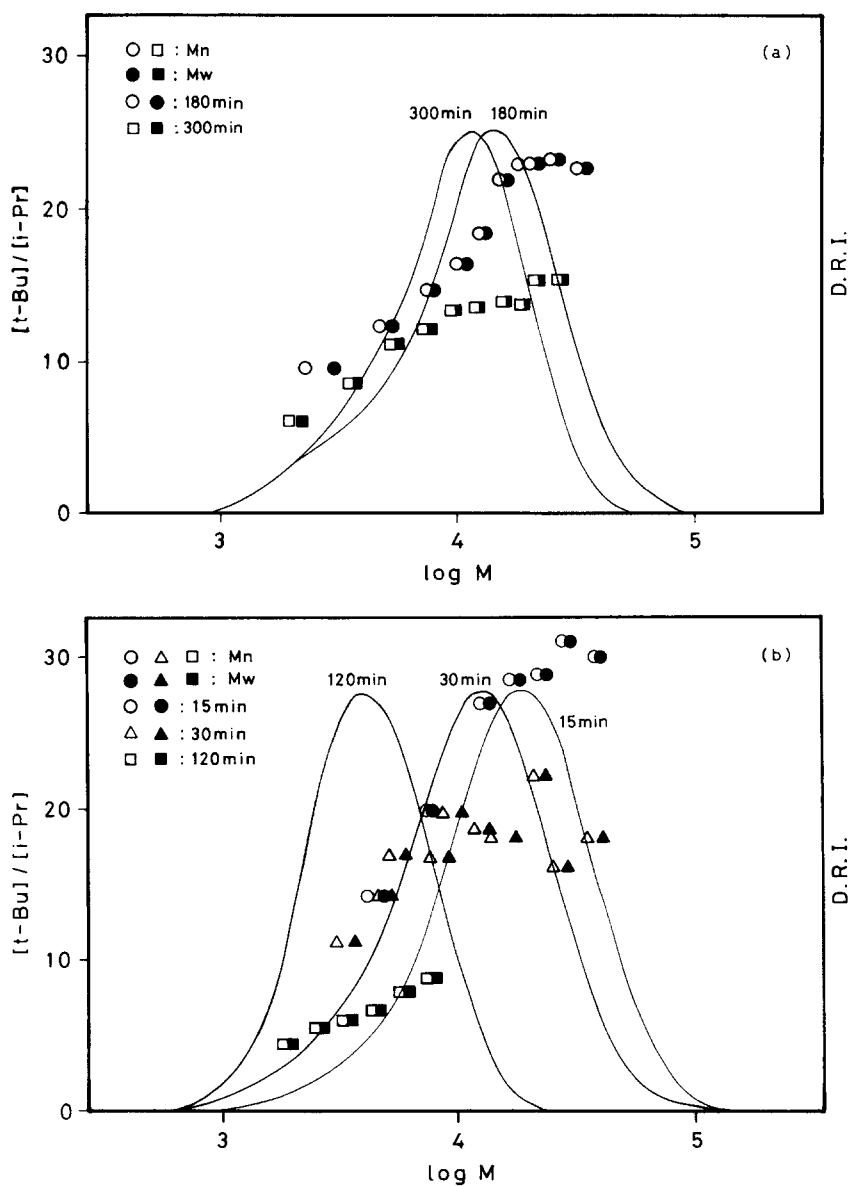


Figure 2 Plots of the composition ratio $[t-Bu]/[i-Pr]$ against M of the fractionated oligomers

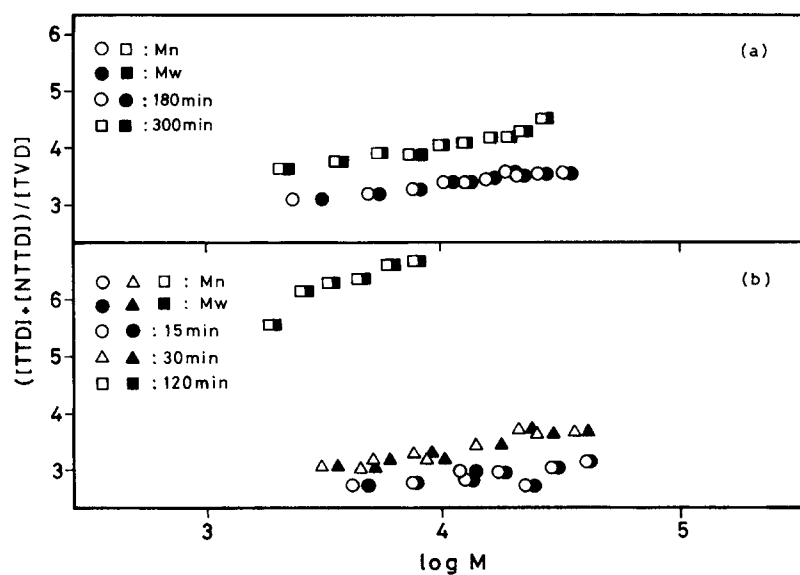


Figure 3 Plots of the composition ratio $((TTD) + [NTTD])/[TVD]$ against M of the fractionated oligomers

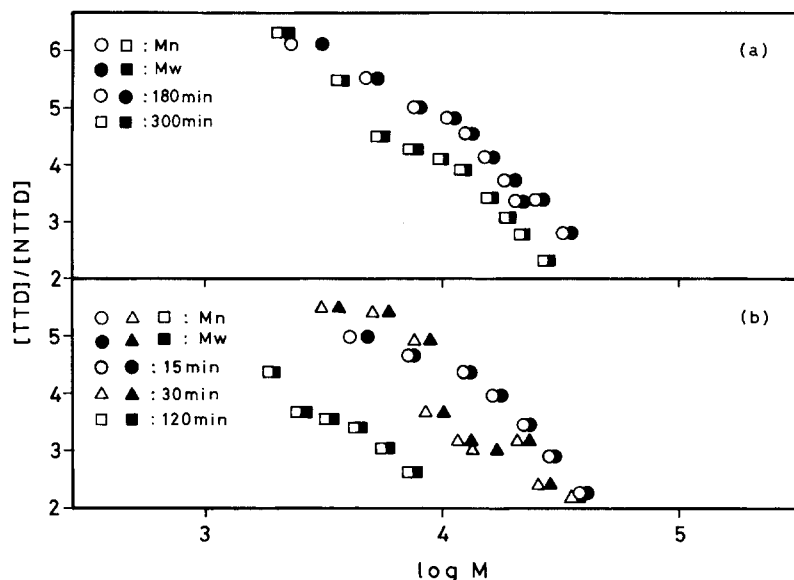


Figure 4 Plots of the composition ratio $[TTD]/[NTTD]$ against M of the fractionated oligomers

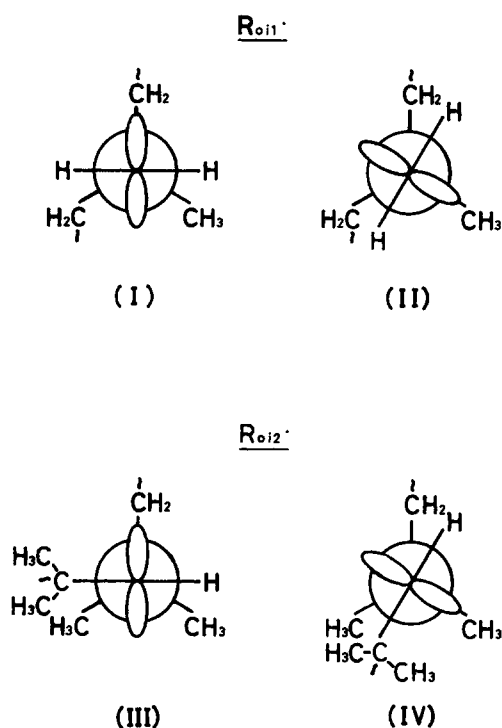


Figure 5 Newman projection diagram of possible rotational isomeric states around the C-C bond of $R_{0i1'}$ and $R_{0i2'}$

The value of exponent a is obtained from the double logarithmic plot of equation (4) by using analytical data for the fractionated oligomers (Tables 1–4). Double logarithmic plots of the ratio $[t\text{-Bu}]/[i\text{Pr}]$ against M of the respective non-volatile oligomers are shown in Figure 6a (300°C) and Figure 6b (320°C). The relationship of equation (4) was verified with a relatively high correlation in the range of M less than about 1×10^4 – 2×10^4 for the respective non-volatile oligomers. Surprisingly, the observed value of exponent a is about 0.5 at 300°C and approaches 0.5 with the reaction time at 320°C. On the other hand, a plateau region having almost unchanged values of the ratio $[t\text{-Bu}]/[i\text{Pr}]$ exists in a range of M higher than about 1×10^4 – 2×10^4 , and the plateau values of $[t\text{-Bu}]/[i\text{Pr}]$ are about 23 and

14 for 180 min and 300 min respectively at 300°C, and about 29 and 18 for 15 min and 30 min respectively at 320°C. For the non-volatile oligomers obtained for 120 min at 320°C, which consist only of molecules having M less than about 1×10^4 , such a plateau region was not observed.

Recently, the molecular weights and temperature dependences of the chain dimensions and the diffusion coefficients of molten polymers have been made determined by small-angle neutron scattering¹⁵ and pulsed-field gradient n.m.r.¹⁶ technique. An unperturbed state of the polymer chain is realized for flexible polymers in the molten state or in a solution of Θ -solvent. It is experimentally and theoretically confirmed^{13,17} that the molecular weight dependence of the zero-shear viscosity of molten polymers is generally given by M^1 for $M < M_c$ and $M^{3.4}$ for $M > M_c$, and that of the self-diffusion coefficient is given by M^1 ($M < M_c$) and M^2 ($M > M_c$), where M_c is the characteristic molecular weight^{18–20}. The value of M_c is estimated to be about three times larger than that of M_e , which is the M value of the onset of entanglement determined from the plateau modulus ($\rho RT/M_e$, where ρ is the density) of linear viscoelasticity¹⁹. The dynamic properties of the unentanglement and entanglement systems could be interpreted by the Rouse model and the reptation model^{13,17}, respectively. In the case of polyisobutylene, the value of M_c is shown to be 1.52×10^4 ¹⁸ and 1.7×10^4 (217°C)²¹ and the value of M_e is 8.9×10^3 ¹⁸, 5.686×10^3 (25°C)²⁰ and 7.288×10^3 (140°C)²⁰. Double logarithmic plots of the zero-shear viscosity against M at 300 and 320°C, which were recalculated using a relationship observed at 217°C²¹, are shown in Figure 6b, together with the values of M_c ²¹ and M_e ²⁰ drawn as dotted lines. For polyisobutylene with M_w ranging from 6.41×10^2 to 1.76×10^6 and with M_w/M_n values of around 1, double logarithmic plots of $[\eta]$ measured in isoamyl isovalerate at 25.0°C (Θ) against M_w follow a straight line with a slope of 0.5²². It is expected that the chain dimension of molten polyisobutylene in the same M range also follows a relationship given by the equation $R \propto M^{0.5}$, where R is the radius of the molten polymer chains.

A schematic illustration of polymer systems of entangled and unentangled polymer chains and a mixed polymer system is shown in Figure 7. In the entangled

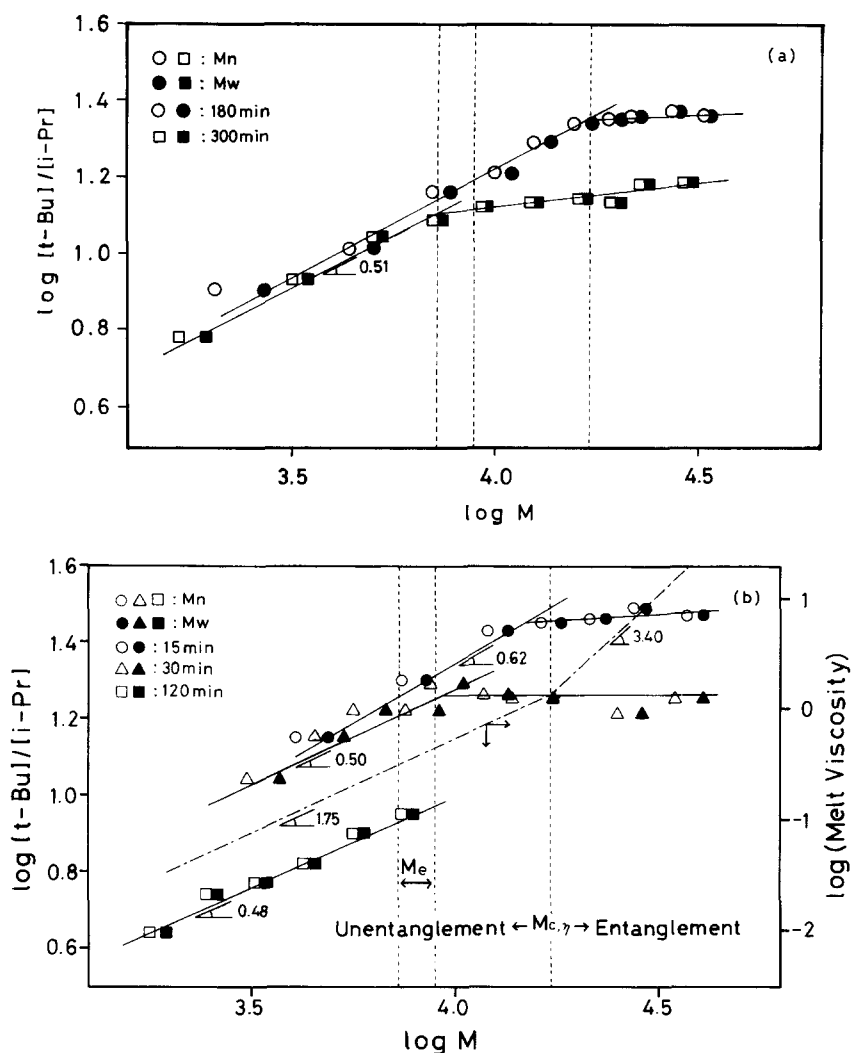


Figure 6 Double logarithmic plots of the composition ratio $[t\text{-Bu}]/[i\text{-Pr}]$ against M of the fractionated oligomers, together with double logarithmic plots of the zero-shear viscosity against M and the values of M_c and M_e drawn by the dotted lines

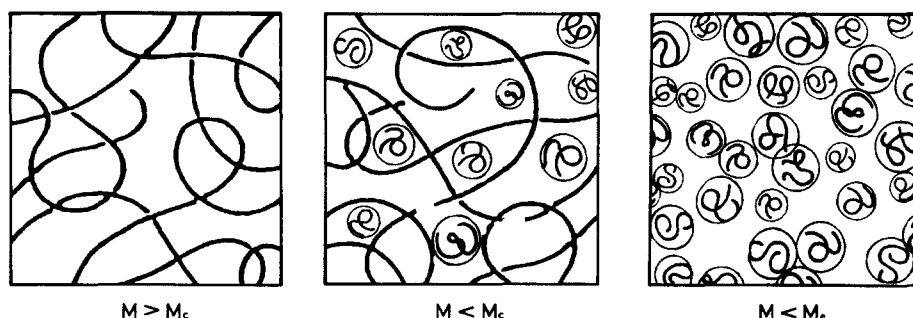


Figure 7 Schematic illustration of the molecular systems in the entangled ($M > M_c$) and the unentangled ($M < M_c$) states, and the mixed polymer system ($M < M_n$)

chains ($M > M_c$), polymer coils interpenetrate each other very strongly. The polymer coils are partially disentangled in the mixed polymer system ($M < M_c$), and the polymer chains are separated from each other as M is less than M_c . Thus, the molten polymer molecules constituting the reaction medium change from the entangled state to the unentangled state through a mixed polymer system as the reaction proceeds. The polymer molecules in these systems would be not phase-separated but would form an homogeneous phase, as is expected from the nearly constant specific volume (V_{sp}) of polyisobutylene at 217°C given by

$$\text{the equation}^{21} V_{sp} = 1.225 + 32/M, \text{ in the range of } M \text{ from } 3.45 \times 10^3 \text{ to } 1.15 \times 10^5.$$

The non-volatile oligomers obtained in the present experiments, except under the conditions of 120 min at 320°C , correspond to the state between the entangled and the mixed polymer systems. Plateau values of $[t\text{-Bu}]/[i\text{-Pr}]$ are observed in the region of M higher than M_c of the respective non-volatile oligomers (Figure 6) and decrease clearly with the degradation time. As described above, this could be interpreted by the simulation results that a larger decrease in $[R_p]$ than in $[R_t]$ results from a large depression

of the regeneration of $R_p\cdot$ in the depropagation step by the decrease in kinetic chain length which in turn is due to an increase in the rate of diffusion-controlled termination with decreasing average molecular weight of the molten polymer matrix¹⁰.

The polymer molecules with $M < M_c$ are disentangled and separated from the entangled molecular chains. The decrease in the ratio $[t\text{-Bu}]/[i\text{Pr}]$ with decreasing M ($M < M_c$) shown in Figure 6a and 6b means a decrease in the radical concentration ratio $[R_p\cdot]/[R_t\cdot]$. It is expected that the concentration of the respective radicals is affected by the difference in the rates of the elementary reactions, depending on the M of the reacting polymer molecules. Mita²³ put forward an idea that the rate of intermolecular hydrogen abstraction of a small radical from a polymer depends on the radius of the random coils of the polymer, assuming that the small radical penetrates into the polymer. This idea is based on the result that the rate constant per monomeric unit of the hydrogen abstraction of the *t*-butoxy radical from polystyrene or polypropylene in a dilute solution is smaller than that from small molecules and decreases with decreasing molecular weight of the polymer²⁴. Thus, it is deduced from the present experiments that the rate constant (k_{si}) of hydrogen abstraction of $S\cdot$ depends on the radius of the polymer molecules. The molecular weight dependence of k_{si} is given by

$$k_{si} \propto R \propto M^{0.5} \quad (5)$$

The intermolecular hydrogen abstraction of $S\cdot$ leads to the formation of semi-volatile oligomers and volatiles, and the on-chain radicals $R_{oi1}\cdot$ and $R_{oi2}\cdot$. As described above, the β scission of $R_{oi1}\cdot$ and $R_{oi2}\cdot$ at the main chain gives terminal double bonds and $R_p\cdot$. In the case of $R_{oi2}\cdot$, NTTD and the methyl radical are formed by β scission at the side methyl group. The radical $S\cdot$ has a volatile molecular size under degradation conditions. Such radicals are methyl radicals, allyl radicals and oligomeric radicals (M_n of about 8×10^2)⁵ including other alkyl radicals, which are formed by the various elementary reactions⁸.

The intermolecular hydrogen abstraction of the respective radicals occurs randomly at any position on the main chain and therefore the polymer concentration should be replaced by the concentration of the monomeric unit $[N]$ of the polymer. $[N]$ is expressed by ρ/m^{25} and could be set almost constant during the degradation²¹, as described above. Under these conditions, the rate equation for the hydrogen abstraction of $S\cdot$ is expressed as follows

$$V_{si} = k_{si}[S\cdot][N] \propto R[S\cdot] \propto M^{0.5}[S\cdot] \quad (6)$$

Thus, the rate of hydrogen abstraction of $S\cdot$ depends on M for $M < M_c$ and the mean concentration $[S\cdot]$ in the homogeneous reaction medium. The mean concentrations $[R_t\cdot]$, $[R_p\cdot]$ and $[S\cdot]$ could be regulated by the average molecular weight of the molten polymer matrix¹⁰, and kept almost constant throughout the molten polymer matrix. The subsequent β scission of the on-chain radicals $R_{oi1}\cdot$ and $R_{oi2}\cdot$ leads to the regeneration of only $R_p\cdot$, not $R_t\cdot$, and the local concentration $[R_p\cdot]_L$ having M less than M_c decreases with decreasing M of each fraction. Thus the M dependences of $[R_p\cdot]_L$ and the concentration ratio $[R_p\cdot]/[R_t\cdot]$ are written as follows

$$[R_p\cdot]_L \propto M^{0.5} \quad (7)$$

$$\frac{[R_p\cdot]}{[R_t\cdot]} \propto \frac{[R_p\cdot]_L + [R_p\cdot]}{[R_t\cdot]} \propto bM^{0.5} + c \quad (8)$$

The observed value of exponent a given by equation (4) for the fractionated oligomers of $M < M_c$ in Figure 6 is consistent with an exponent 0.5 for M given by equation (5). This result indicates that the rate of intermolecular hydrogen abstraction of $S\cdot$ depends on the chain dimension of unentangled polymer molecules, being proportional to R of the molecular chain.

On the other hand, the hydrogen abstraction of $S\cdot$ from the entangled molecular chains is independent of M for $M > M_c$, although the molecular weight dependence of R is also evaluated by $M^{0.5}$. The radical $S\cdot$ is incorporated into the network of entanglement, where the concentration of segments having abstracting hydrogen atoms is kept almost constant in the molten polymer matrix. Thereby, $S\cdot$ cannot recognize the individual molecular chain and abstracts randomly a hydrogen atom of a segment of any molecule. In this M region, the elementary reactions are not affected by the chain dimension of the molecule owing to an entanglement effect of the segment concentration, but are affected by the segmental motion for the rotation-dependent β scission¹¹ and by the self-diffusional motion for the diffusion-controlled termination¹⁰.

CONCLUSIONS

The effects of the molecular weight of molecular chains constituting the reaction medium on the thermal degradation of polyisobutylene were examined in terms of the distribution of functional groups of the oligomers fractionated from the non-volatile oligomers obtained at 300 or 320°C. In particular, the effects of the dynamic properties of the entangled and the unentangled molten polymer system on their formation were discussed with regard to the intermolecular hydrogen abstraction of $R_p\cdot$, $R_t\cdot$ and $S\cdot$, followed by β scission. The observed value of the composition ratio $[\text{TTD}]/[\text{NTTD}]$ increases monotonically with decreasing M of the fractions. This result shows clearly that the reactivity for β scission depends on the segmental motion of the reacting radicals. The composition ratio $[t\text{-Bu}]/[i\text{Pr}]$ is roughly constant for M higher than the characteristic molecular weight M_c in the unentangled and the entangled polymer system, but decreases with a decrease in M for $M < M_c$. This ratio for $M > M_c$ decreases with decreasing average molecular weight of the molten polymer matrix, owing to an increase in the rate of diffusion-controlled termination¹⁰. For $M < M_c$, the value of the exponent a determined from the double logarithmic plots of $[t\text{-Bu}]/[i\text{Pr}]$ against M is about 0.5. This result is interpreted using the concept that the hydrogen abstraction of $S\cdot$ depends on the chain dimension of unentangled polymer. These results indicate that the degradation reaction of polymer molecules in an homogenous reaction medium is entirely affected by segmental motion for the rotation-dependent β scission¹¹, and by self-diffusional motion for the diffusion-controlled termination¹⁰. On the other hand, the effect of the chain dimension of the molecules on the intermolecular hydrogen abstraction of $S\cdot$ was observed only for the unentangled polymer molecules during the degradation.

REFERENCES

- (a) Benson, S. W. and North, A. M., *J. Am. Chem. Soc.*, 1959, **81**, 1139. (b) Mahadad, H. K. and O'Driscoll, K. F., *J. Polym. Sci., Polym. Chem.*, 1977, **15**, 1175. (c) Horie, K. and Mita, I., *Polym. J.*, 1977, **9**, 201.

2. (a) Horie, K. and Mita, I., *Macromolecules*, 1978, **11**, 1175. (b) Mita, I., Horie, K. and Takada, M., *Macromolecules*, 1981, **14**, 1428. (c) Strukelj, M., Martinho, M. G., Winnik, M. A. and Quirk, R. P., *Macromolecules*, 1991, **24**, 2488.
3. Mita, I. and Horie, K., in *Degradation of and Stabilization of Polymers*, ed. H. H. G. Jellinek. Elsevier, New York, 1983, Chapter 5.
4. Mita, I., in *Aspects of Degradation and Stabilization of Polymers*, ed. H. H. G. Jellinek. Elsevier, New York, 1978, Chapter 6.
5. Sawaguchi, T., Tekesue, T., Ikemura, T. and Seno, M., *Macromol. Chem. Phys.*, 1995, **196**, 4139.
6. Sawaguchi, T., Ikemura, T. and Seno, M., *Macromol. Chem. Phys.*, 1996, **197**, 215.
7. Sawaguchi, T. and Seno, M., *Polym. J.*, 1996, **28**, 392.
8. Sawaguchi, T. and Seno, M., *Polymer*, 1996, **37**, 3697.
9. Sawaguchi, T., Ikemura, T. and Seno, M., *Polymer*, 1996, **37**, 5411.
10. Sawaguchi, T. and Seno, M., *Polymer*, 1996, **37**, 5607.
11. Sawaguchi, T. and Seno, M., *Polym. Deg. Stab.*, 1996, **54**, 23.
12. Sawaguchi, T. and Seno, M., *Polym. Deg. Stab.*, 1996, **54**, 33.
13. (a) de Gennes, P. G., *Scaling Concepts in Polymer Physics*. Cornell University Press, New York, 1979. (b) Doi, M. and Edwards, S. F., *The Theory of Polymer Dynamics*, Clarendon Press, Oxford, 1986. (c) Nagasawa, M. (ed.), *Molecular Conformation and Dynamics of Macromolecules in Condensed System*. Elsevier, New York, 1988.
14. Sakaguchi, Y. and Sakurada, I., *Kobunshi Kagaku*, 1948, **5**, 242.
15. (a) Higgins, J. S. and Stein, R. S., *J. Appl. Cryst.*, 1978, **11**, 346. (b) Hayashi, H., Flory, P. J. and Wignall, G. D., *Macromolecules*, 1983, **16**, 1328. (c) Vacatello, M., Yoon, D. Y. and Flory, P. J., *Macromolecules*, 1990, **23**, 1993. (d) Boothroyd, A. T., Rennie, A. R. and Boothroyd, C. B., *Europhys. Lett.*, 1991, **15**, 715.
16. (a) von Meerwall, E. D., *Adv. Polym. Sci.*, 1983, **42**, 288; *Rubber Chem. Technol.*, 1985, **58**, 527. (b) Karger, J., Pfeifer, H. and Heink, W., *Adv. Magn. Reson.*, 1988, **12**, 1.
17. (a) Tirrell, M., *Rubber Chem. Technol.*, 1984, **57**, 523. (b) Antonietti, M., Coutandin, J. and Sillescu, H., *Macromolecules*, 1986, **19**, 793. (c) Green, P. F. and Kramer, E. J., *Macromolecules*, 1986, **19**, 1108. (d) Pearson, D. S., Strate, G. V., von Meerwall, E. and Schilling, F. C., *Macromolecules*, 1987, **20**, 1133. (e) Nemoto, N., Kishine, M., Inoue, T. and Osaki, K., *Macromolecules*, 1991, **24**, 1648. (f) Pearson, D. S., Fetters, L. J., Graessley, W. W., Strate, G. V. and von Meerwall, E., *Macromolecules*, 1994, **27**, 711.
18. Graessley, W. W., *Adv. Polym. Sci.*, 1974, **16**, 1.
19. Ferry, J. D., *Viscoelastic Properties of Polymer*. John Wiley and Sons, New York, 1980.
20. Fetters, L. J., Lohse, D. J., Richter, D., Witten, T. A. and Zirkel, A., *Macromolecules*, 1994, **27**, 4639.
21. Fox, T. G. and Flory, P. J., *J. Phys. Colloid Chem.*, 1951, **55**, 221.
22. (a) Abe, F., Einaga, Y. and Yamakawa, H., *Macromolecules*, 1991, **24**, 4423. (b) Abe, F., Einaga, Y. and Yamakawa, H., *Macromolecules*, 1993, **26**, 1891.
23. Mita, I., *High Polym. Jpn.*, 1978, **27**, 595.
24. (a) Niki, E. and Kamiya, Y., *J. Org. Chem.*, 1973, **38**, 1403. (b) Niki, E. and Kamiya, Y., *J. Chem. Soc. Perkin Trans. II*, 1975, 1221.
25. (a) Cameron, G. G., *Makromol. Chem.*, 1978, **100**, 255. (b) Cameron, G. G., Meyer, J. M. and McWalter, I. T., *Macromolecules*, 1978, **11**, 696.